Lévy-type diffusion on one-dimensional directed Cantor graphs

Raffaella Burioni,[1,2] Luca Caniparoli,[1] Stefano Lepri,[3] and Alessandro Vezzani[4,1]
[1]*Dipartimento di Fisica, Università degli Studi di Parma, Viale G.P. Usberti 7/A, 43100 Parma, Italy*
[2]*INFN, Gruppo Collegato di Parma, Viale G.P. Usberti 7/A, 43100 Parma, Italy*
[3]*Istituto dei Sistemi Complessi, Consiglio Nazionale delle Ricerche, via Madonna del Piano 10, I-50019 Sesto Fiorentino, Italy*
[4]*CNR-INFM S3, Dipartimento di Fisica, Università di Modena e Reggio Emilia, Via G. Campi 213A, 41000 Modena, Italy*
(Received 8 October 2009; published 21 January 2010)

Lévy-type walks with correlated jumps, induced by the topology of the medium, are studied on a class of one-dimensional deterministic graphs built from generalized Cantor and Smith-Volterra-Cantor sets. The particle performs a standard random walk on the sets but is also allowed to move ballistically throughout the empty regions. Using scaling relations and the mapping onto the electric network problem, we obtain the exact values of the scaling exponents for the asymptotic return probability, the resistivity, and the mean-square displacement as a function of the topological parameters of the sets. Interestingly, the system undergoes a transition from superdiffusive to diffusive behavior as a function of the filling of the fractal. The deterministic topology also allows us to discuss the importance of the choice of the initial condition. In particular, we demonstrate that local and average measurements can display different asymptotic behavior. The analytic results are compared to the numerical solution of the master equation of the process.

DOI: 10.1103/PhysRevE.81.011127 PACS number(s): 05.40.Fb, 02.50.Ey, 05.60.−k

I. INTRODUCTION

Stochastic processes characterized by Lévy walks are relevant in many physical phenomena ranging from condensed matter, biological systems, and ecology to transport in turbulent fluids and in porous media. In recent years, there has been a growing interest in the field (see Ref. [1] for a recent overview). However, direct comparison of theoretical predictions to experimental data in fully controlled experimental conditions is often unfeasible. As a matter of fact, evidence of anomalous transport and diffusion is often indirect and experimental setups allowing a direct and tunable study of such phenomena are hardly available. A breakthrough in the field was achieved in a recent experiment by means of an engineered material where light rays were demonstrated to perform a Lévy-walk type of diffusion [2]. This new class of materials is built by packing glass microspheres with diameters following a Lévy distribution and then filling the space between the spheres with strongly scattering nanoparticles. As light is not scattered within the microspheres, anomalous diffusion arises as a consequence of the power-law distribution of their diameters. The results of the experiments were indeed interpreted using a model of Lévy walks [3,4] for photons and the new material was named *Lévy glass*. An important feature of the experimental samples is that the walk is correlated and the correlation is induced by the topology of the quenched medium. Light that has just crossed a large glass microsphere without being scattered has a high probability of being backscattered at the subsequent step undergoing a jump of similar size. Studies on models of Lévy flights have evidenced that spatial correlations in jump probabilities have a deep influence on the diffusion properties [5–7]. Here, however, we consider Lévy walk models, where particles either move ballistically or are scattered by impurities, and do not perform long-range instantaneous flights. Recently, one-dimensional models for Lévy walks, where the correlation is induced by an underlying quenched and correlated random environment, have been studied. One-dimensional models represent simplified systems and may not compare quantitatively to real experiments. Nevertheless they allow for an exact solution of the dynamics. The recent studies focused, respectively, on the mean-square displacement in a Lévy-Lorentz gas [8] and on the conductivity and transmission through a chain of barriers with Lévy-distributed spacings [9]. Interestingly, in simple random walks, these different aspects are not independent and they can be connected by assuming standard scaling relations for the random-walk probabilities [10] and exploiting the analogy between the associated master equation and the Kirchhoff equations [11]. When an analogous scaling holds for Lévy walks, then it can be applied to relate the scaling exponents of the return probability, the mean-square displacement, and the effective resistance of the samples. Another subtle point in random models is represented by the choice of the starting site, as discussed in Ref. [8], and it would be interesting to have a direct control on this problem.

In this paper, we will present a new class of one-dimensional models for correlated Lévy walks, which will allow us to investigate in detail the scaling and the relation between transmission and mean-square displacement, as well as the dependence on the starting point through average and local diffusion properties. More specifically, we will consider diffusion across deterministic fractals, namely, generalized Cantor and Cantor-Smith-Volterra sets (the latter being the simplest examples of fat fractals). The walker dynamics is such that it performs a standard random-walk step on sites belonging to the set, while moving ballistically (without changing direction) otherwise. In the following, we will refer to these two types of sites as "bidirectional" or "unidirectional," respectively. Lévy-type diffusion may thus arise as the longer steps will be distributed according to the voids of the Cantor set, much in the same spirit of the Lévy glass experiment [2].

The model can be mapped onto a random walk on a suitable directed graph and it allows to obtain analytical results

by extending the usual scaling arguments. In particular, the scaling of the resistivity with the length of the graph yields the exponents for the asymptotics of the return probability and the mean-square displacement. Interestingly, the system undergoes a transition from superdiffusive to diffusive behavior as a function of the density of the fractal. A similar transition has already been evidenced for Lévy flights in presence of quenched noise [6] and also in the model of Ref. [9].

A subtle effect of quenched disorder is the dependence of the observables on the choice of the walker starting site [8]. An insight on this issue is clearly relevant for guiding experimental investigations. Due to the simple deterministic topology, our model allows for a clear analysis of such issue. In particular, the choice of a random starting point corresponds to a measure of quantities averaged over all possible starting sites. On inhomogeneous structures, such averages can display a different asymptotic behavior [12] with respect the corresponding local quantities, obtained by taking into account a specific starting point. This is indeed the case for generalized Cantor sets: scaling relations hold for local quantities but are violated for average ones. In particular, in the local case, the random walker shifts from a superdiffusive to a diffusive motion, as a function of topological parameters tuning the void density. In the average case, the behavior is even richer: a change of the void density and size induces a transition among three different regimes characterized by ballistic, superdiffusive, and standard diffusive motions, respectively. In this case, which appears to be the closest to the experimental settings, adopting a method similar to Ref. [8], we give a rigorous bound on the mean-square displacement and discuss the violation of scaling relations.

The paper is organized as follows. In Sec. II, we introduce the topology and the dynamics of the model. In Sec. III, we first review the scaling relations connecting random-walk properties and the resistivity and derive the exact results for the resistivity and for the local asymptotic behavior of the walker itself. We also check, via the numerical solution of the master equation, the scaling hypothesis for local quantities. In Sec IV, we turn to the average case and provide a rigorous lower bound for the exponent of the mean-square displacement as a function of the distribution of the voids. We show under which condition the bound is fulfilled exactly. Also in this case, we compare our analytical results to the numerical solution of the master equation. Some concluding remarks are given in Sec. V.

II. RANDOM WALKER ON GENERALIZED CANTOR GRAPHS

A. Random walk across Cantor sets

The standard Cantor set is built by removing the middle thirds of a linear chain and iterating the rule in every segment. The resulting set has zero measure, with fractal (Hausdorff) dimension $d_f^{(set)}=\frac{\log 2}{\log 3}$. The procedure can be easily generalized: let us denote by n_s the number of parts in which we split the segment (n_s odd). Removing parts in even positions and iterating the process, the measure of the remaining set is still zero and its fractal dimension is

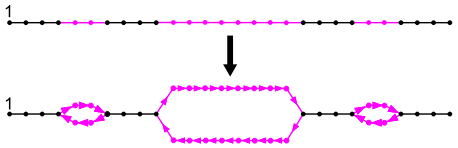

FIG. 1. (Color online) (Upper figure) The discrete Cantor set in gray (fuchsia); the sites which have been removed (voids). (Lower figure) The Cantor graph associated to the Cantor set at generation $G=3$ where undirectional bubbles have been introduced to describe ballistic motion in the voids. The site $i=1$ is the origin of the graph.

$$d_f^{(set)}=\frac{\log\frac{n_s+1}{2}}{\log n_s}. \tag{1}$$

If one builds the Cantor set by growing the fractal, then in this notation, $n_r=\frac{n_s+1}{2}$ is the number of replicas of the generation $G-1$ in the generation G. The integer n_r will be used in the following to identify a given set. One can introduce the discrete version of the above procedure, as in the upper part of Fig. 1, where the dark sites represent the Cantor set and the gray (fuchsia) sites have been removed and correspond to voids.

Let us now introduce a random walker on such family of Cantor set. The walker can reside on any site of the lattice. If it is on the void regions, it moves ballistically without changing direction: when the random walker enters a void from left (right), it keeps going left (right) without being scattered until it reaches the opposite edge of the void itself. If instead the walker is on the sites belonging to the Cantor set, it performs a standard random walk with 1/2 probability to move right or left at the next step.

Denoting with $P_{ij}^{\pm}(t)$ the probability that a walker started at site i arrives at time t at site j, respectively, with positive or negative velocity ($i=1,\ldots,N_{tot}$ can be both a site of the Cantor set or a void site, see upper part of Fig. 1), then the master equation of the corresponding process reads

$$\begin{aligned} P_{ij}^{+}(t+1)&=T_{j-1}P_{ij-1}^{+}(t)+(1-T_{j-1})P_{ij-1}^{-}(t),\\ P_{ij}^{-}(t+1)&=(1-T_{j+1})P_{ij+1}^{+}(t)+T_{j+1}P_{ij+1}^{-}(t). \end{aligned} \tag{2}$$

The Cantor structure is therefore defined by the transmission coefficients

$$T_j=\begin{cases} 1/2, & \text{if } j \text{ is on the Cantor set}\\ 1, & \text{on the voids.}\end{cases} \tag{3}$$

The above choice for T_j yields indeed a ballistic motion on the voids and a random-walk behavior on the Cantor set. The choice $T_j=T$ is readily recognized to correspond to the standard persistent random walk [13]. In this respect, our model can also be regarded as a random walk with a site-dependent persistence (see, e.g., [14] and references therein).

B. Cantor graphs from Cantor sets

Let us introduce an equivalent approach based on graph theory. We associate to the Cantor set a directed *Cantor*

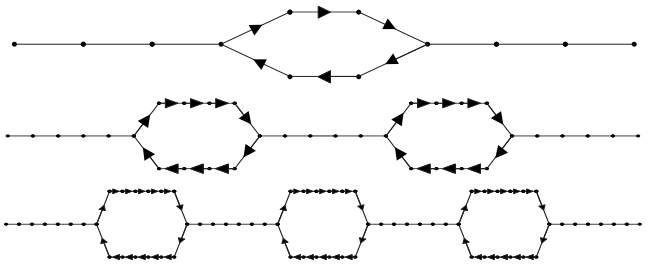

FIG. 2. Three examples of Cantor graphs of generation 2 with $n_r=2,3,4$.

graph, obtained by putting undirected links in every "solid" segment and replacing the voids with bubbles of appropriate length whose sites are connected by directed links (see Fig. 1 for an explicit construction). Some examples of graphs at different n_r are shown in Fig. 2. In this framework, the model consists of a random walk on such a directed graph. The adjacency matrix A_{ij} of the graph is defined as $A_{ij}=A_{ji}=1$ if sites i and j are connected by an undirected link, $A_{ij}=1$ if the site i is connected to site j by a link directed from i to j and 0 otherwise. The outgoing coordination number $z_i=\Sigma_j A_{ij}$ is 1 in the voids and 2 in the solid segments. The transition probability for the random walk is therefore $p_{ij}=A_{ij}/z_i$.

The structure of the voids in the Cantor graph strongly influences the motion of the random walker, so let us now introduce a further generalization. In the previous examples, the lengths L_k of the unidirectional segments are $L_k=n_s^k$, $k=1,\ldots,G-1$, where G is the generation of the graph. However, we can choose an arbitrary n_u (n_u integer ≥ 2) so that the length of the unidirectional segments becomes

$$L_k = n_u^k, \quad k = 1, \ldots, G-1, \tag{4}$$

as is shown in Fig. 3.

From Eq. (4), we can compute $N_b(G,n_r)$ and $N_u(G,n_r,n_u)$, the number of bidirectional and unidirectional sites, respectively (those plotted in black and fuchsia in Fig. 1), in a graph of generation G,

$$N_b = 2n_r^G \tag{5}$$

$$N_u = \begin{cases} \dfrac{(n_u-1)n_r^G-(n_r-1)n_u^G}{n_r-n_u}+1 & \text{if } n_u \neq n_r \\ -n_r^G+(n_r-1)Gn_r^{G-1}+1 & \text{if } n_u = n_r. \end{cases} \tag{6}$$

Accordingly, the total number of sites is $N_{tot}(G,n_r,n_s)$ is

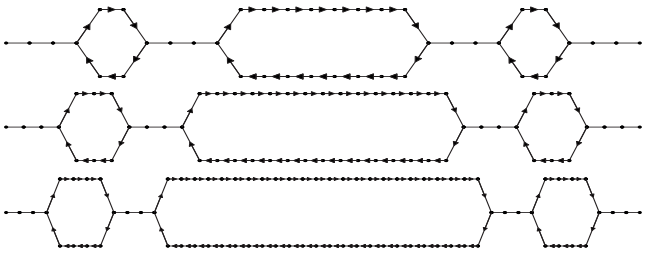

FIG. 3. The generation $G=3$ of the graph with $n_u=3,4,5$ in the $n_r=2$ case.

$$N_{tot} = \begin{cases} \dfrac{(2n_r-n_u-1)n_r^G-(n_r-1)n_u^G}{n_r-n_u}+1 & \text{if } n_u \neq n_r \\ n_r^G+(n_r-1)Gn_r^{G-1}+1 & \text{if } n_u = n_r. \end{cases} \tag{7}$$

From Eqs. (5)–(7), it follows that the measure of both sets N_b and N_u is strictly positive if $n_u<n_r$. This choice of the parameters corresponds to the so-called *fat* fractals. An example of this kind of structure is the Smith-Volterra-Cantor set. Conversely, we will name *slim* fractals the graphs with $n_u>n_r$, where the measure of the solid segments is vanishing.

It is important to notice that, even if the Cantor set has a fractal dimension $d_f^{(set)}<1$, Eq. (1), the directed Cantor graph has always a fractal dimension $d_f=1$. Indeed, since the voids have been filled with one-dimensional bubbles, the number of sites within a distance r from a given site grows as $\sim r^{d_f}$, with $d_f=1$.

III. DIFFUSION ON CANTOR GRAPHS: LOCAL BEHAVIOR

A. Asymptotic properties of random walks, spectral dimensions, and Einstein relations

On the directed Cantor graph, we can now define the standard random-walk quantities. Their asymptotic behaviors are expected to be described by power laws, with characteristic exponents, usually related only to the large-scale topology of the structure [12].

Let $P_{ij}(t)$ be the probability that a walker started at site i arrives at j in t steps, $P_{ij}(t)=P_{ij}^+(t)+P_{ij}^-(t)$. In particular, $P_{ii}(t)$ is the random-walk autocorrelation function, i.e., the return probability to the starting point after t steps. At large times t, it is expected that [15]

$$P_{ii}(t) \sim t^{-d_s/2}, \tag{8}$$

where d_s often coincides with the spectral dimension, which also rules the low eigenvalues region of the spectrum for the discrete Laplacian on the graph [16]. In the case at hand, being the graph directed, d_s simply describes the asymptotic behavior of the return probability, but we will refer to it as a "generalized" spectral dimension as well [17–19].

The mean-square displacement from the starting site i after t steps is

$$\langle x_i^2\rangle - \langle x_i\rangle^2 \equiv \left(\sum_j x_{ij}^2 P_{ij}(t)\right) - \left(\sum_j x_{ij} P_{ij}(t)\right)^2, \tag{9}$$

where x_{ij} is the distance between the sites i and j. If the starting site corresponds to the origin of the Cantor graph ($i=1$ in Fig. 1) and periodic boundary conditions are chosen, as in all our numerical solutions, then $\langle x_i\rangle=0$ for symmetry reasons. The exponent γ defined by the asymptotic behavior

$$\langle x_i^2\rangle \sim t^{\gamma} \tag{10}$$

classifies the diffusive properties of the random walker: $\gamma=1$ corresponds to usual diffusion, $\gamma>1$ to superdiffusion, and $\gamma<1$ is typical of a subdiffusion. The value $\gamma=2$ char-

acterizes a ballistic motion where the random walker displacement grows linearly with time.

It is well known that on regular structures, the dynamic exponents ruling the return probability and the mean-square displacement are not independent, i.e., for systems where scaling holds [10]

$$\gamma = d_s/d_f. \tag{11}$$

In the Appendix, we will show that such a relation still holds under a generalized scaling hypothesis that takes into account the underlying fractal structure of the Cantor graph. More precisely, we assume that $P_{ij}(t)$ depends on j only through the distance $x_{ij} \equiv r$, between i and j, i.e., $P_{ij}(t) \equiv P_i(r,t)$ and that

$$P_i(r,t) = t^{-d_s/2} f_i\left\{\frac{r}{\ell(t)}, g[\log_x \ell(t)]\right\}, \tag{12}$$

where $\ell(t)$ is the correlation length of the system and $g(\cdot)$ is a periodic function of a logarithm in arbitrary base x. The master function f_i can depend on the initial site. The scaling factor $t^{-d_s/2}$ ensures consistency with the definition of the return probability, Eq. (8), as seen by setting $j=i$ $(r=0)$ in Eq. (12). Moreover, log-periodic oscillations are superimposed to the leading exponential behavior as it is expected on fractals [20]. In the Appendix, we also show that, up to log-periodic corrections, $\langle x_i^2 \rangle \sim \ell^2(t)$ and that

$$\ell(t) = t^{d_s/2d_f}. \tag{13}$$

In general, $P_i(r,t)$ presents the above scaling form for large-enough times. In our calculations, we verified that if the walker starts from the origin of the structure, scaling is realized in a few steps. A different choice can give rise to very long transients where $P_{ij}(t)$ may also depend on the direction and not only on the distance r alone. The net effect is a nonvanishing drift $\langle x_i(t) \rangle \neq 0$ for short times.

A simple analogy between the master equation of the random walk and the Kirchhoff equations [11] allows to associate to each directed graph a network of resistors (see again the Appendix). In this framework, it is possible to compute analytically the exponent α describing the growth of the resistance Ω as a function of the distance r between contacts, i.e., $\Omega \sim r^{\alpha}$. Exploiting Eq. (12), one can prove also the following Einstein relation:

$$\alpha = \frac{2d_f}{d_s} - d_f. \tag{14}$$

For local quantities and exponents, we can thus use Eq. (14) to calculate d_s. We will verify it numerically, also testing the validity of the scaling hypothesis.

B. Local spectral dimension

When scaling holds, the local spectral dimension can be obtained using the scaling law of the resistance Ω and the relation (14). In the network of resistors associated to the Cantor graph, every bidirectional link has resistance 1, while for unidirectional links, a *whole* bubble has unit resistance (see the Appendix). The resistance between the extremes of the structure of generation G can be evaluated using the recurrence relation

$$\Omega(G,n_r) = n_r \Omega(G-1,n_r) + (n_r - 1).$$

Using the initial condition $\Omega(1,n_r) = 2n_r - 1$, one has

$$\Omega(G,n_r) = 2n_r^G - 1. \tag{15}$$

Expressing Ω as a function of the distance r between contacts at generation G, in the $G \to \infty$ asymptotic limit, we obtain the exponent α and, via the scaling relation (14), the value of d_s, ruling the return probability and the mean-square displacement

$$d_s = \begin{cases} \dfrac{2}{1 + \dfrac{\log n_r}{\log n_u}}, & \text{if } n_u > n_r \\ \dfrac{2}{2 - \dfrac{\log\log r}{\log r}}, & \text{if } n_u = n_r \\ 1 & \text{if } n_u < n_r \end{cases} \tag{16}$$

and $\gamma = d_s$, where we have used that $d_f = 1$. Interestingly, the system exhibits a transition from a superdiffusive to a normally diffusive regime at $n_u = n_r$. The random walker on the slim Cantor graphs experiences a superdiffusive regime while it presents a normal diffusion on fat structures, with logarithmic corrections in the critical case $n_u = n_r$. Intuitively, slim Cantor graphs mainly consist of long unidirectional bubbles, which lead to a superdiffusive behavior, while in the opposite case, the bubbles practically disappear and hence one could expect a normal diffusion.

C. Numerical results: The master equation and generalized scaling

For a simple and effective numerical study of the system, we solved iteratively the master equation Eq. (2) with initial condition $P_{ij}^{\pm}(0) = \delta_{ij}/2$ and periodic boundary conditions. We first tested the dynamical scaling of the probability density (12), considering for $g(\cdot)$ a periodic function with unit period in $\log_{n_u}[\ell(t)]$, so that the log-periodicity takes into account the self similarity of the underlying structure. It is thus convenient to look at the data at constant $g[\log_{n_u} \ell(t)]$, namely, as prescribed by Eqs. (13) and (16), at successive times

$$t_k = t_0 [n_u n_r]^k. \tag{17}$$

Figures 4 refers to a slim and a fat structure. For the former case the scaling is reasonably accurate, although the convergence to the asymptotic shape is not complete. Moreover the two panels show that for different sequences of times satisfying relation (17) (i.e., different t_0) the scaling function changes, evidencing that the introduction of a generalized scaling with a log-periodic term is necessary in this situation. The scaling function also depends on the starting site i, while the exponent are site independent. For the fat case, the curves tend to be closer and closer to a Gaussian, confirming that the diffusion is normal. Times have not to be chosen accord-

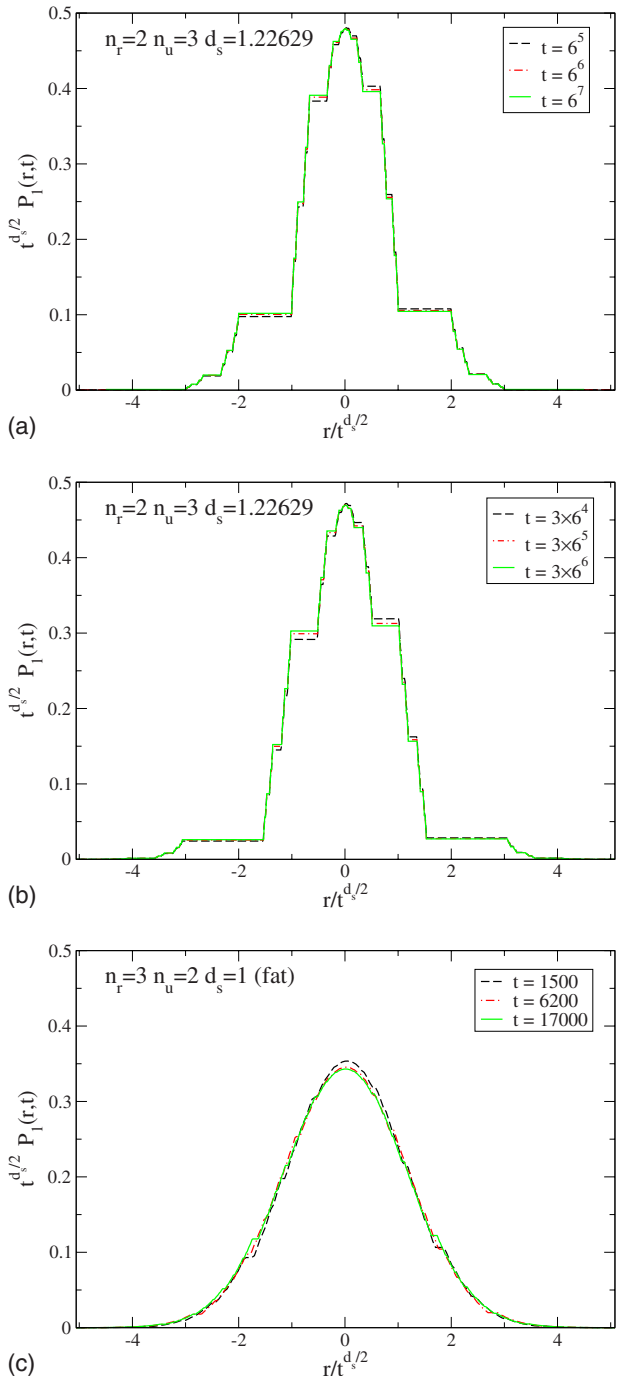

FIG. 4. (Color online) Dynamical scaling of the probability for initial site $i=1$. The sizes of the lattices correspond to generations $G=9,9,8$, respectively.

ing to Eq. (17) since in this case log-periodic oscillations are not present.

Figures 5 and 6 demonstrate that the probability of return $P_{ii}(t)$ and the mean-square displacement behave asymptotically (up to log-periodic corrections) as prescribed by Eqs. (8), (10), and (16) ($d_f=1$ for all Cantor graphs). Indeed, power-law fits of the curves give exponents 1.21, 1.13, and 1.03 which are in excellent agreement with the theoretical values of d_s, Eq. (16) ($d_s=1.2262,\ldots,1.115\,77,\ldots,1$, respectively).

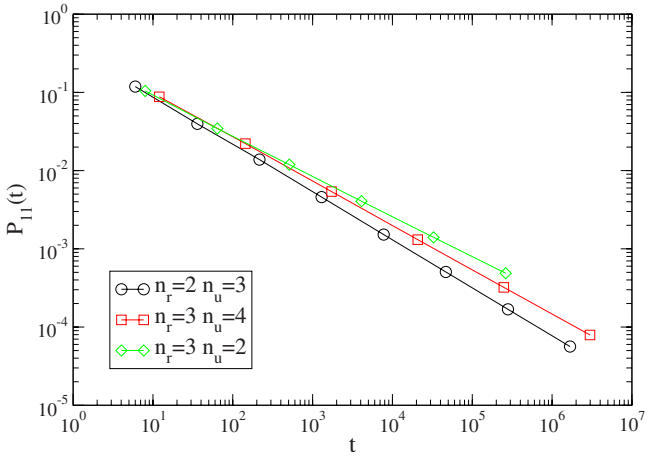

FIG. 5. (Color online) Dynamical scaling of the probability for initial site $i=1$. Lattices of size N_{tot} correspond to $G=9,7,8$, respectively. To avoid the big jumps and zeros, what is actually plotted is a coarse-grained probability $\Sigma_{t=t_{k-1}}^{t_k} P_{ii}(t)/[t_k-t_{k-1}]$.

IV. DIFFUSION ON CANTOR GRAPHS: AVERAGE BEHAVIOR

The exponents characterizing the asymptotic behavior of random walks are in general independent of the starting site i even on inhomogeneous structures. However, due to inhomogeneity, averages over the starting points can result in radically different asymptotic behaviors with respect to local case [12]. It is thus necessary to introduce some further averaging on the initial conditions. Let S_k (k integer) be a sequence of subgraphs ($S_k \subset S_{k+1}$) covering the infinite graph. We define the average mean-square displacement

$$\overline{\langle x^2 \rangle} = \lim_{k\to\infty} \frac{1}{N_k} \sum_{i \in S_k} \langle x_i^2 \rangle \tag{18}$$

(N_k is the number of sites in S_k) and the average return probability

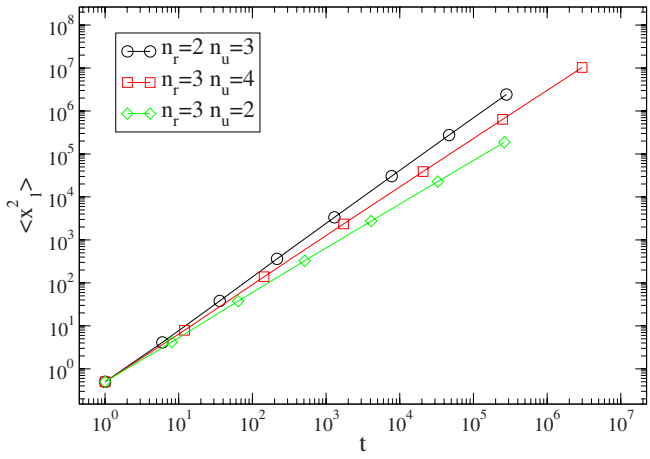

FIG. 6. (Color online) Growth of the mean-square displacements for initial site $i=1$. Lattices of size N corresponding to $G=9,7,8$, respectively.

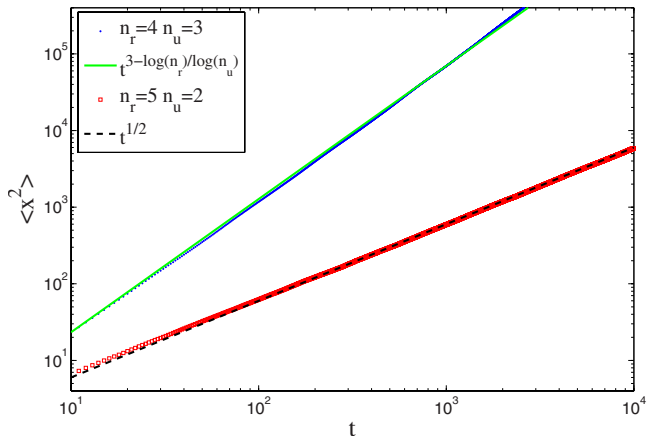

FIG. 7. (Color online) Average mean-square displacement, as defined in Eq. (18), for the fat fractals with $n_r=4$, $n_u=3$ and $n_r=5$, $n_u=2$. Solid and dashed lines are the superdiffusive, Eq. (25), and diffusive behaviors expected in the two structures, respectively.

$$\overline{P(t)} = \lim_{k\to\infty} \frac{1}{N_k} \sum_{i \in S_k} P_{ii}(t). \tag{19}$$

Interestingly, due to the fact that the thermodynamic limit does not commute with the large time limit, the average quantities ((18) and (19)) can feature a different asymptotic behavior with respect to their local counterparts. Therefore, as done for the local case, Eqs. (8) and (10), we introduce the exponents $\bar{d}_s$ and $\bar{\gamma}$ for the average quantities

$$\overline{P(t)} \sim t^{-\bar{d}_s/2}, \quad \overline{\langle x^2 \rangle} \sim t^{\bar{\gamma}}. \tag{20}$$

On the Cantor graph, average exponents not only differ from the local ones, but also they do not satisfy relations (11) and (14). Indeed, for average quantities, scaling is violated and the topology of the graph influences diffusion in a highly nontrivial way. Diffusion is ballistic on slim ($n_u > n_r$) Cantor graphs, while on fat graphs, even if d_s always equals 1, there are two different scenarios

$$\bar{\gamma} = \begin{cases} 3 - \dfrac{\log n_r}{\log n_u}, & \text{if } n_u < n_r < n_u^2 \\ 1 & \text{if } n_u^2 < n_r. \end{cases} \tag{21}$$

In both cases, we obtain a lower bound for the average mean-square displacement and then we check numerically that this lower bound is satisfied when $n_r < n_u^2$, obtaining the exponent given in Eq. (21).

In analogy with [8], let us study the probability $P_b(l)$ to take a first ballistic step of length $>l$. We will show that, on slim Cantor graphs, this probability approaches 1 when $G \to \infty$ for every l and the motion is therefore ballistic on average. On the other hand, on fat Cantor graphs, the limit is a finite number going to 0 for $l \to \infty$ with a characteristic power law. Let us consider the unidirectional segments of length greater than l: the "favorable" sites in a unidirectional segment of length $L_k > l$ are $L_k - l$ and we have to sum over k. Recalling that the number of segments of length $L_k = n_u^k$ is $(n_r-1)n_r^{G-1-k}$, we can write $P_b(l)$ as

$$P_b(l) = \lim_{G\to\infty} \frac{\sum_{k=k_0}^{G-1} (n_u^k - 1 - l)(n_r - 1)(n_r)^{G-1-k}}{N_{tot}(G, n_s, n_u)}, \tag{22}$$

where k_0 is an integer chosen such that $n_u^{k_0} > l$, i.e., $k_0 := \lceil \frac{\log(l)}{\log n_u} \rceil$ (reminding that $\lceil x \rceil := \min\{n \in \mathbb{Z} | n \geq x\}$ is the ceiling function) and $N_{tot}(G, n_r, n_u)$ is the total number of sites in the graph of generation G, given in Eq. (7). The series in the numerator of (22) can be summed and we obtain

$$P_b(l) = \lim_{G\to\infty} \frac{1}{N_{tot}} \left\{ \frac{n_r - 1}{n_u - n_r} n_u^G + \left[\frac{n_r - 1}{n_r - n_u} \left(\frac{n_u}{n_r} \right)^{k_0} - (1 + l) n_r^{-k_0} \right] n_r^G + (1 + l) \right\}.$$

Therefore, we have two exponential terms with different bases: the leading term for $G \to \infty$ will then be different depending on n_r and n_u.

If $n_u > n_r$ (i.e., on a slim Cantor graph), considering the asymptotic behavior of $N_{tot}(G, n_r, n_u)$ in Eq. (7), one obtains

$$P_b(l) = \lim_{G\to\infty} \frac{-n_u^G (n_r - 1) + o(n_u^G)}{-n_u^G (n_r - 1) + o(n_u^G)} = 1.$$

Thus, the probability of going through a ballistic step of length $>l$ is 1 for every l and the walker behaves ballistically on average.

Let us now consider the same limit in the case $n_u < n_r$. Omitting the ceiling function in k_0 (it can be done with a suitably chosen l), we have

$$P_b(l) \sim \left(\frac{n_r}{n_u} \right)^{-k_0} = l^{1 - \log n_r / \log n_u}. \tag{23}$$

In order to estimate the average mean-square displacement in the fat case, let us introduce the average probability of being at distance r after t steps as $\bar{P}(r,t)$. It is convenient to split it in two parts writing

$$\bar{P}(r,t) = \bar{P}^*(r,t; r < t) + \frac{P_b(t)}{2} [\delta(r - t) + \delta(r + t)], \tag{24}$$

where P_b is the average probability of performing t consecutive ballistic steps and $\bar{P}^*(r,t;r<t)$ is the average probability of arriving in t step at r after some scatterings. Equation (24) provides a lower bound for the mean-square displacement

$$\overline{\langle x^2 \rangle} = \int_0^\infty dr r^2 \bar{P}(r,t) > \int_0^\infty dr r^2 \frac{P_b(t)}{2} [\delta(r - t) + \delta(r + t)] \sim t^{3 - \log n_r / \log n_u}, \tag{25}$$

where we used expressions (23) for $P_b(t)$. For $1 < \frac{\log n_r}{\log n_u} < 2$, the inequality (25) proves that the system is superdiffusive and $\overline{\langle x^2 \rangle} \sim t^{3 - \log n_r / \log n_u}$ is expected to be the correct asymptotic behavior of the average mean-square displacement. In Fig. 7, we compare our analytical prediction to numerical data, showing an excellent agreement [21]. For

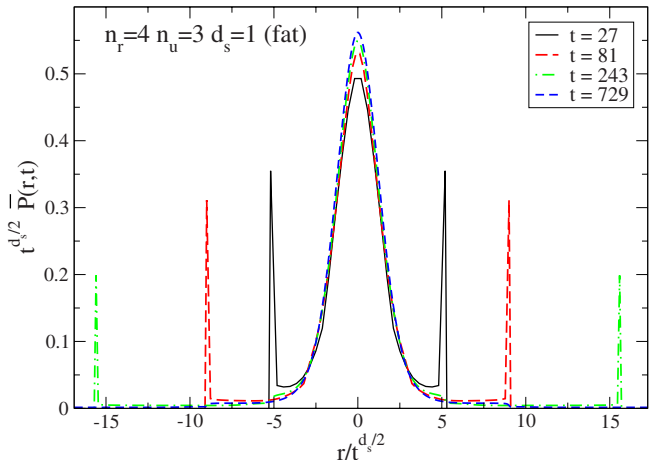

FIG. 8. (Color online) Dynamic scaling of the averaged probability $\bar{P}$ with $n_r=4$ and $n_u=3$ lattices of size $N_{tot}=58\,976$ ($G=7$). The average is on all initial sites.

$\frac{\log n_r}{\log n_u} > 2$, inequality (25) is trivial and a normal diffusion is expected since the ballistic stretch does not provide a significant contribution to $\overline{\langle x^2 \rangle}$. The presence of normal diffusion in this case is also evidenced in Fig. 7.

Figure 8 shows that, in the fat case, there are actually two different contributions to $\bar{P}(r,t)$: a ballistic peak lowering with t and a central peak which scales as in normal diffusion. This behavior clearly breaks the scaling hypothesis (12) and relations (11) and (14) between exponents do not hold. Indeed, for $\log(n_r)/\log(n_u) < 2$, $\bar{\gamma} = 3 - \frac{\log n_r}{\log n_u}$, while $\bar{d}_s = 1$ and $\bar{\alpha} = 1$.

V. CONCLUSIONS

The recent experiments on light scattering in disordered materials open the way to direct and tunable measurements on systems performing Lévy walks. The quenched disorder in the experimental samples has been engineered in order to obtain a specific effects and the geometry induces a correlation in Lévy walks. In this paper, we take a first step in understanding the influence of geometry in these disordered samples by studying a one-dimensional structure obtained from the generalization of Cantor and Cantor-Smith-Volterra sets, where a random walker performs steps that are both Lévy distributed and correlated. Although the applicability of such idealized one-dimensional models to real experiments is not granted, much theoretical insight can be obtained from their solution. Using an exact mapping to an equivalent directed graph for the process, we determine the asymptotic behavior for the return probability and the mean-square displacement and study the validity of the Einstein relations in the local and average case.

From our results, it appears that the average case is the closest to the real experimental setting [2] and further analysis in higher dimensions are currently under consideration. An important point is that experimental samples do contain a certain degree of disorder, which must be taken into account in order to understand to what extent it can affect diffusion properties.

ACKNOWLEDGMENTS

We acknowledge useful discussions with D. ben-Avraham, P. Barthelemy, J. Bertolotti, R. Livi, D. S. Wiersma, and K. Vynck. This work is partially supported by the CNR RSTL Project No. 827 *Dinamiche cooperative in strutture quasi uni-dimensionali*.

APPENDIX

In this appendix, we show that the Einstein relation Eq. (14) between different exponents is a direct consequence of the generalized scaling hypothesis, Eq. (12). Since $P_{ij}(t)$ is a probability, its sum over all sites n is normalized to one at every time t. Moreover, in the scaling hypothesis, all the spatial dependences are encoded by the distance $x_{ij} \equiv r$, therefore such a sum can be evaluated by introducing an integral in $Kr^{d_f-1}dr$, where d_f is the fractal dimension and K is a suitable constant, obtaining

$$t^{-d_s/2} \int f_i \left\{ \frac{r}{\ell(t)}, g[\log_x \ell(t)] \right\} K r^{d_f-1} dr = 1. \tag{A1}$$

Changing the integration variable to $r/\ell(t)$, we have

$$t^{-d_s/2} \ell^{d_f}(t) G(t) = 1, \tag{A2}$$

where $G(t)$ is a log-periodic function. Equation (A2) is satisfied if $G(t)=1$ and if Eq. (13) holds.

To derive Eq. (11), let us consider the mean-square displacement

$$\langle x_i^2(t) \rangle = t^{-d_s/2} \int r^2 f_i \left\{ \frac{r}{\ell(t)}, g[\log_x \ell(t)] \right\} K r^{d_f-1} dr \tag{A3}$$

Upon choosing again the new integration variable $r/\ell(t)$, we have

$$\langle x_i^2 \rangle = \ell^2(t) G_1(t) = t^{d_s/d_f} G_1(t), \tag{A4}$$

where $G_1(t)$ is a log-periodic function.

Let us finally consider the equation for the electric potential V_i on a network of unitary resistors where a unitary current flows from site 0 to site n and we have

$$-\sum_j L_{ji} V_j = \delta_{i0} - \delta_{in}, \tag{A5}$$

where $L_{ij} = z_i \delta_{ij} - A_{ij}$ is the Laplacian matrix. Notice that according to Eq. (A5), in a directed Cantor graph, the inner links of a bubble are short circuit and a whole bubble has resistance one. In the framework of random walks on directed Cantor graph, the master equation (2) can be recasted as

$$P_{0i}(t+1) - P_{0i}(t) = -\sum_j L_{ji} P_{0j}(t)/z_j + \delta_{i0}\delta_{t0}. \tag{A6}$$

Denoting with $\tilde{P}_{0i}(\omega)$ the Fourier transform of $P_{0i}(t)$, we get

$$\tilde{P}_{0i}(\omega)(e^{i\omega} - 1) = -\sum_j L_{ji} \tilde{P}_{0j}(\omega)/z_j + \delta_{i0} \tag{A7}$$

comparing Eqs. (A5) and (A7)

$$V_i = \frac{1}{z_i}\lim_{\omega\to 0}[\tilde{P}_{0i}(\omega) - \tilde{P}_{ni}(\omega)]. \quad \text{(A8)}$$

The potential difference between sites 0 and n as a function of their distance r can be, hence, obtained introducing in $\lim_{\omega\to 0}\tilde{P}_{0n}(\omega)$ the scaling relation Eq. (12)

$$V(r) \sim \lim_{\omega\to 0}\int dt\, e^{i\omega t} t^{-d_s/2} f_i\left\{\frac{r}{\ell(t)}, g[\log_x \ell(t)]\right\}. \quad \text{(A9)}$$

Changing the variable of integration into $t' = \omega t$, we get

$$V(r) \sim r^{2d_f/d_s - d_f}\lim_{\omega\to 0} G_3\left\{\frac{r}{\tilde{\ell}(\omega)}, g[\log_x \tilde{\ell}(\omega)]\right\}, \quad \text{(A10)}$$

where G_3 is a suitable function and $\tilde{\ell}(\omega) = \omega^{-d_s/(2d_f)}$ is the correlation length in terms of the frequency ω. Therefore, Eq. (14) holds.

[1] *Anomalous Transport: Foundations and Applications*, edited by R. Klages, G. Radons, and I. M. Sokolov (Wiley, Berlin, 2008).

[2] P. Barthelemy, J. Bertolotti, and D. S. Wiersma, Nature (London) **453**, 495 (2008).

[3] A. Blumen, G. Zumofen, and J. Klafter, Phys. Rev. A **40**, 3964 (1989).

[4] J. Klafter, A. Blumen, G. Zumofen, and M. F. Shlesinger, Physica A **168**, 637 (1990).

[5] H. C. Fogedby, Phys. Rev. Lett. **73**, 2517 (1994).

[6] R. Kutner and P. Maass, J. Phys. A **31**, 2603 (1998).

[7] M. Schulz, Phys. Lett. A **298**, 105 (2002).

[8] E. Barkai, V. Fleurov, and J. Klafter, Phys. Rev. E **61**, 1164 (2000).

[9] C. W. J. Beenakker, C. W. Groth, and A. R. Akhmerov, Phys. Rev. B **79**, 024204 (2009).

[10] M. E. Cates, J. Phys. (Paris) **46**, 1059 (1985).

[11] P. G. Doyle and J. L. Snell, *Random Walks and Electric Networks* (The Mathematical Association of America, Inc., Washington, D.C., 1999).

[12] R. Burioni and D. Cassi, J. Phys. A **38**, R45 (2005).

[13] G. H. Weiss, *Aspects and Applications of the Random Walk* (North-Holland, Amsterdam, 1994).

[14] M. Miri, Z. Sadjadi, and M. E. Fouladvand, Phys. Rev. E **73**, 031115 (2006).

[15] S. Alexander and R. Orbach, J. Phys. (Paris), Lett. **43**, L625 (1982); K. Hattori, T. Hattori, and H. Watanabe, Prog. Theor. Phys. **92**, 108 (1987).

[16] R. Burioni and D. Cassi, Phys. Rev. Lett. **76**, 1091 (1996).

[17] D. ben-Avraham and S. Havlin, *Diffusion and Reactions in Fractals and Disordered Systems* (Cambridge University Press, London, 2004).

[18] F. Harary, *Graph Theory* (Addison-Wesley, Reading, MA, 1969).

[19] J. J. Kozak and V. Balakrishnan, Phys. Rev. E **65**, 021105 (2002).

[20] P. J. Grabner and W. Woess, Stochastic Proc. Appl. **69**, 127 (1997).

[21] In Fig. 7, we introduce a correction in order to evaluate averages on infinite graphs. Let $\overline{\langle x^2\rangle}_G$ be the mean-square displacement evaluated at the generation G. Then we have $\overline{\langle x^2\rangle} = \overline{\langle x^2\rangle}_G(1-P_G) + t^2 P_G$, where P_G is the probability of being at time $t=0$ in a bubble larger than the largest bubble of G on the infinite graph. Clearly, we expect that such a correction is valid only for time much smaller than the size of this largest bubble. Indeed only in this case the average motion for walkers starting on such bubbles can be considered purely ballistic.